Energy & Buildings 353 (2026) 116898

Contents lists available at ScienceDirect

Energy & Buildings

journal homepage: www.elsevier.com/locate/enb

Quantum computing approach for building surface sunlit in urban-scale energy modeling

Zhipeng Deng [a,*], Yujie Xu [b], Tianzhen Hong [b]

[a] Department of Mechanical and Aerospace Engineering, College of Engineering and Computer Science, University of Central Florida, Orlando, FL, USA
[b] Building Technology and Urban Systems Division, Lawrence Berkeley National Laboratory, Berkeley, CA, USA

ARTICLE INFO

Keywords:
Quantum annealing
Binary optimization
Hidden surface detection
Möller-Trumbore intersection algorithm
Solar shadow calculation
Solar energy

ABSTRACT

Solar shadow calculations are needed in building energy modeling and performance simulation of PV systems installed on roofs or facades of buildings. We present a quantum computing approach for calculation of building surface sunlit fractions by recasting solar visibility as a binary optimization problem solved by quantum annealing. Each triangulated surface centroid is encoded as a binary qubit indicating sunlit or shaded status. Geometric visibility constraints are derived from the Möller-Trumbore intersection algorithm and converted into a constrained quadratic binary model compatible with contemporary quantum annealers. The coefficients were embedded to D-Wave quantum computer. To demonstrate feasibility, we conducted a case study in San Francisco for a target building with 52 triangles and roughly 2700 nearby triangles within 50 m evaluated at representative winter and summer solar positions. The results demonstrated that quantum annealing can reliably calculate and distinguish sunlit from shaded surfaces. Quantum samples achieved average accuracy exceeding 92.4 %, with the aggregate surface-level agreement approaching 99.9 %. The outputs of quantum computers agreed closely with classical algorithms, indicating practical feasibility and promising scalability. Finally, the hourly sunlit fractions of building surfaces can be obtained for urban energy modelling. This is the first study to apply quantum computing to the solar shadow and building surface sunlit calculation. It introduces a new paradigm that differs fundamentally from traditional approaches.

1. Introduction

1.1. Background of surface sunlit fractions

1.1.1. Importance of solar distribution calculation

Buildings are responsible for about one-third of global energy consumption and a quarter of carbon dioxide emissions [1]. Solar radiation is one of the most influential factors in building science and sustainable urban design and simulation [2]. It serves both as a renewable source of energy and as a primary driver of thermal loads that affect energy use and occupant comfort in buildings [3,4]. Harnessing this energy effectively is essential for high-performance building design.

In colder climates, solar radiation can provide passive heating, reducing dependence on fossil fuel-based systems [5]. Adequate daylighting not only lowers artificial lighting needs but also improves occupant productivity and well-being [6]. Direct sunlight exposure can lead to localized overheating, and glare, negatively impacting occupant comfort [3]. This dual nature of solar radiation, offering both benefits and drawbacks, highlights the need for precise solar exposure analysis in architecture and urban planning.

To inform decision making in urban energy planning, it requires designing and operating urban buildings as a group rather than as single individuals, accounting for interactions among buildings [7]. Accurate calculation of solar shadows on building exterior surfaces is of great importance in whole building energy modeling, especially in dense urban areas where buildings shade each other [8,9]. Building thermal load and energy simulation requires the calculation of the shadows caused by the built environment, building elements or shading devices based on the certain angle of incidence of the sun relative to the surface being considered [10]. One widely used metric is the sunlit fraction, the proportion of a surface directly illuminated by the sun at a given moment [11]. This fraction varies with time of day, season, and local obstructions [12]. High-resolution estimates of the sunlit fraction are critical for predicting thermal loads, HVAC sizing, daylighting potential, and renewable energy yield.

* Corresponding author.
E-mail address: zhipeng.deng@ucf.edu (Z. Deng).

https://doi.org/10.1016/j.enbuild.2025.116898
Received 18 October 2025; Received in revised form 7 December 2025; Accepted 20 December 2025
Available online 26 December 2025
0378-7788/

1.1.2. Challenges

Determining solar shading at the urban scale is a computationally demanding task. Each surface in a city model can both cast and receive shadows. For every time step in the simulation, the model must check for obstructions between the sun and each point of interest [13]. As the number of surfaces increases, the number of potential shadow-casting interactions grows rapidly, creating a substantial computational burden [6,14,15].

Accurate annual performance or photovoltaic potential assessments require shading calculations for numerous solar positions, often hourly or sub-hourly, throughout the year (over 8760 time steps). This temporal complexity compounds the already demanding geometric checks. Moreover, precise shadow boundaries require fine spatial discretization, increasing the number of calculation points [12]. The situation becomes even more complex when including vegetation. Capturing these dynamics may require advanced representations like voxel models or LiDAR-derived point clouds [16,17]. Finally, large-scale simulations depend on vast datasets, such as high-resolution LiDAR scans or 3D city models (e.g., CityGML) [18,19]. Efficiently processing and performing geometric operations on these datasets with thousands of buildings requires substantial memory and specialized algorithms. Scaling these methods from small neighborhoods to entire cities is a major challenge, often tackled using parallel computing or GPU acceleration [20,21].

1.1.3. Motivation for using quantum computing to compute sunlit fraction

The computational challenges outlined above highlight the need for fundamentally new approaches to urban-scale solar simulation. Even with advances in high-performance computing and graphics processing units (GPUs), scaling shading calculations to citywide models with fine spatial and temporal resolution remains resource-intensive and, in some cases, impractical for real-time applications [12,22]. The problem is characterized by large, combinatorial sets of geometric relationships between many surfaces, which grow exponentially as model size increases.

Quantum computing offers a promising avenue to address these challenges. By leveraging quantum parallelism, entanglement, and superposition, certain classes of geometric and visibility problems could be reformulated as efficiently solvable on quantum hardware, potentially reducing computation times from hours to minutes [23]. Quantum algorithms designed for spatial search, graph analysis, and optimization could be adapted to rapidly evaluate shadow-casting relationships among thousands of surfaces across multiple time steps [24]. Moreover, hybrid quantum–classical workflows could integrate quantum speedups with existing building performance simulation (BPS) pipelines, enabling previously infeasible urban-scale shading analyses without sacrificing model fidelity.

In this paper, we explore the feasibility of using quantum computing to calculate the sunlit fraction of building surfaces in dense urban environments. We aim to bridge the gap between the geometric complexity of shading analysis and the emerging capabilities of quantum algorithms, demonstrating how this paradigm shift could support more accurate, scalable, and energy-conscious urban design practices.

1.2. Literature review

1.2.1. Traditional solar distribution calculation methods

Accurately computing the sunlit fraction of building surfaces has been a longstanding challenge in BPS and urban energy modeling [25,26]. Over the years, several methods have evolved from simple analytic approaches to sophisticated algorithms that leverage modern GPU acceleration.

(a) Early shading methods, like Trigonometric Methods (TgM) and vector-based shadow casting, are efficient for simple geometries [27], failing to capture complex 3D features.
(b) Projection and Clipping (PgC) is a common “object-space” method in BPS tools like EnergyPlus. PgC is accurate for simple, convex polygons but struggles with complex, non-convex shapes [28].
(c) Image-space GPU approaches is significantly faster for complex urban scenes, robustly handling arbitrary geometries (irregular, curved, perforated), and is now a high-performance option in tools like EnergyPlus, enabling next-generation BPS and UBEM [14,21].
(d) GPU ray tracing approach is another “scene-based” technique [29]. It simulates light photons by “shooting” parallel rays from a source. Ray tracing naturally handles semi-transparent materials by respawning rays with reduced energy, making it robust for complex geometries and urban-scale modeling [6,15,30].
(e) Voxel-based methods discretize 3D urban space into volumetric “voxels,” assigning properties (empty, building, vegetation). This is effective for complex volumes like tree canopies [31,32].
(f) GIS-based district level solar shadow models have been developed to estimate the solar potential of a building group, including simplified geometry calculations [33–35] and stochastic models with image processing [36]. Moreover, researchers also developed machine learning and deep learning tools to estimate solar shadow in recent years [22,37,38].

While modern GPU and voxel approaches can handle complex scenes, they remain compute-intensive for city-scale, time-resolved simulations, requiring billions of intersection tests annually [25]. This motivates exploration into quantum computing techniques, which promise fundamental speedups for certain classes of geometric and light-transport problems.

1.2.2. Quantum computing methods

The shift to ray tracing methods in solar distribution calculation is driven by the development of high-performance parallel computing infrastructure, making large-scale urban building energy modeling and rendering practical. As an emerging computational technique, the advances in quantum computing pose new opportunities to further accelerate these demanding computations. In the literature, there are three main paradigms of approaches in applying quantum computing to ray tracing: unstructured search, numerical integration, and light transport simulation.

The first paradigm frames ray casting as an unstructured search problem, applying Grover’s algorithm to find ray-primitive intersections [39–41]. These methods treat the collection of N geometric primitives in a scene as an unordered list [40]. The ray casting problem is then defined as a search for the index i of a primitive p_i that satisfies two conditions: (1) the ray r intersects a geometry primitive p_i, and (2) the intersection point is the closest one to the ray’s origin among all possible intersections. While this offers a theoretical quadratic speedup to $O(\sqrt{N})$ over a naive classical linear scan $O(N)$, it is asymptotically slower than modern classical ray tracers that can achieve $O(logN)$ performance [42] by employing spatial acceleration structures like kd-tree [43]. Furthermore, these methods are mainly demonstrated on simulators rather than on actual quantum computers, except [39] presented a simplified case with parallel and axis-aligned rectangles and rays orthogonal to the surfaces with integer coordinates. This line of work is challenging to implement on real quantum computers due to the high circuit complexity for even trivial cases [39].

The second paradigm reframes rendering as a high-dimensional numerical integration problem, leveraging quantum amplitude estimation to achieve a quadratically improved error convergence rate over classical Monte Carlo methods, promising faster convergence [44]. The core principle involves preparing a quantum state where the target integral is encoded in the amplitude of one of the basis states. Then, using techniques related to Quantum Phase Estimation and the Quantum Fourier

Transform, the algorithm can estimate this amplitude. The result is a quadratic improvement in the error convergence rate of classical Monte Carlo, from $O(1/\sqrt{N})$ to $O(1/N)$ using the quantum technique [44]. This suggests that quantum rendering could produce images with far less noise for the same number of queries or achieve the same quality with quadratically fewer queries.

The third and most ambitious paradigm attempts to directly simulate the physics of light transport using quantum random walks, proposing a method to evaluate an exponential number of light paths in polynomial time. A quantum state is constructed to represent the position and direction of a "quantum ray." The evolution of this state, governed by a set of unitary operators that encode the scene's geometry and material properties, mimics the process of light transport. Because a quantum system can exist in a superposition of states, a single execution of the quantum random walk can simulate an exponential number of different light paths simultaneously. This allows for the preparation of a final quantum state that is a superposition of an exponential number of complete light transport paths using only polynomial-time quantum resources [42].

Most previous studies remain quantum simulator-based, with real quantum hardware implementations restricted to trivial geometries. The potential of quantum annealing for ray-casting problems has not been explored, and the feasibility of these methods for dense, realistic urban shading scenarios is untested. This work aims to address these gaps.

To solve problems using quantum annealing, we applied the principle of adiabatic evolution. Initially, the quantum system is prepared in the lowest energy eigenstate of a simple Hamiltonian, known as the driver Hamiltonian [45]. The system then evolves according to a time-dependent total Hamiltonian $H(s)$, where the annealing parameters gradually change from s = 0 to s = 1. The specific form of this total Hamiltonian is designed for problems that can be mapped to the Ising model shown below. This Hamiltonian represents the energy landscape of interacting qubits, which are the basic units of information in quantum computing

$$H(s) = -\frac{A(s)}{2}\sum_i \widehat{\sigma}_x^{(i)} + \frac{B(s)}{2}\left(\sum_i h_i \widehat{\sigma}_z^{(i)} + \sum_{i>j} J_{ij}\widehat{\sigma}_z^{(i)}\widehat{\sigma}_z^{(j)}\right) \tag{1}$$

where $\widehat{\sigma}$ was Pauli matrices operating on a qubit q_i, $A(s)$ the tunneling energy at annealing fraction s, $B(s)$ the Problem Hamiltonian energy at annealing fraction s, h_i the self-interaction energy on a qubit. J_{ij} the coupling energies between spins. The total Hamiltonian $H(s)$ is critically composed of two competing parts. Driver Hamiltonian is represented by the first term. This term typically involves Pauli operators acting on each qubit. It promotes quantum tunneling and exploration of the configuration space. Problem Hamiltonian is represented by the second term. This term encodes the specific optimization problem we aim to solve. It is operating on a system of interacting with qubits or spins.

Quantum annealing has attracted significant attention for its unique capabilities, offering advantages over traditional computers in both computational methods and speed. Based on the principles of quantum mechanics, it uses qubits to perform calculations, enabling faster solutions to complex problems [46,47]. Because of qubit superposition, adding more qubits can exponentially accelerate the solution of complex problems involving many variables. Recent advancements in quantum annealers and algorithms have further expanded the ability to address highly complex optimization challenges, including NP-hard problems [48]. To use quantum annealing for building surface sunlit calculation, the problem must first be reformulated into a quadratic unconstrained binary optimization form as

$$H(\boldsymbol{x}) = \sum_i C_i x_i + \sum_{i,j} C_{ij} x_i x_j \tag{2}$$

where x_i is optimized binary variables, C_i and C_{ij} are linear and quadratic coefficients, respectively. Then we could map the problem into the quantum annealer to solve.

In recent years, there are several quantum computing applications for energy systems [49], such as HVAC system [50], data center [51], power grid [52,53], and electric vehicle charging [54]. However, it has not been used for solar shadow and building surface sunlit calculation.

Here is a brief overview of the remaining sections. Section 2 introduces the detailed methodology, including formulation of solar shadow problem, quantum computing approach, a case study in San Francisco, and quantum computer configuration. Section 3 presents the results, highlighting the status of qubit and surface results in two days. Section 4 discusses the broader implications of the study. Section 5 concludes with the key findings.

2. Methods

Fig. 1 illustrates the overall methodology. We used the actual urban building geometry model of city of San Francisco, California, USA [55]. All the surfaces were Delaunay triangulated, allowing us to extract both vertex and centroid coordinates of triangular surfaces. The solar angles were obtained from the typical meteorological year (TMY) file of San Francisco. We then formulated the problem as a binary optimization, where the objective and constraints were defined such that the status of each surface either sunlit or shaded was represented as a binary variable as qubit. This formulation enabled efficient solution using a quantum annealer. The python code for quantum algorithm includes head command, optimized variables, objective, constraints, and output command. For running the quantum computer, the steps are as follows: upload data and programs to Leap quantum cloud, configuration (annealing time, QPU architecture, qubit states, model, solver etc.), minor embedding, and run quantum annealer. As a result, we obtained detailed solar shadow outcomes, which can be directly applied in urban scale energy simulations.

2.1. Formulation of surface sunlight

Before computation, the sunlight status of a surface can be described using the quantum superposition of qubits. Specifically, a surface can simultaneously exist in both possible states, sunlit and shaded, until measurement collapses the quantum system. This binary status is naturally represented using qubits as

$$|\alpha\rangle = a|\mathrm{light}\rangle + b|\mathrm{shadow}\rangle \tag{3}$$

Here $|\,\rangle$ is Dirac notation for qubit state, and a, b are real coefficients satisfying the normalization condition $a^2 + b^2 = 1$. Eq (3) means the quantum state of mathematical entity in quantum physics [56]. Our objective is to determine the correct state for each surface, given its three-dimensional position and the direction of incoming solar rays.

Fig. 2 shows the illustration of 3D triangular surface interacting with solar rays when determining whether the centroid of a triangular lies in sunlight or shadow. A triangular surface in space is defined by vertices p_1, p_2, p_3 and

$$p_i = (x_i, y_i, z_i) \tag{4}$$

The solar ray is assumed to be parallel, and the direction is given in the form of a vector defined as

$$L = (l_x, l_y, l_z) \tag{5}$$

For the centroid point of the target triangle surface in space $X(x,y,z)$, we must determine whether the solar ray from the source to X intersects with any other triangular surface in space. To solve this solar shadow problem, we employed the Möller-Trumbore intersection algorithm [57]. If an intersection occurs and lies between the light source and centroid X , then the light is blocked, and X is in shadow. And the opposite is not.

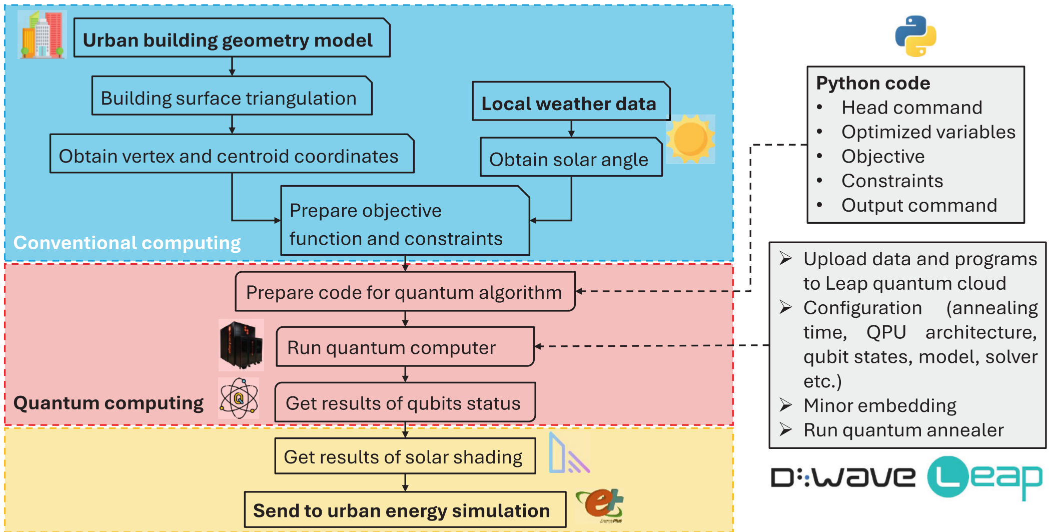

Fig. 1. Overview of methodology of quantum computing approach for building surface sunlit calculation.

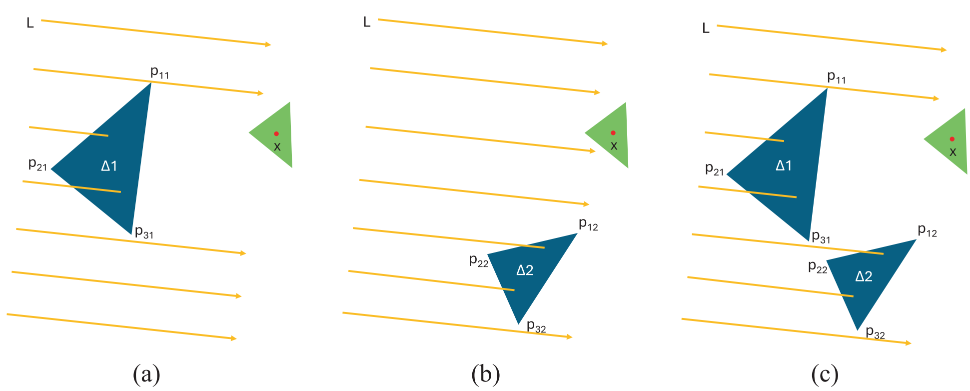

Fig. 2. Illustration of 3D triangular surface interacting with solar rays when determining whether the centroid of a triangular lies in sunlight or shadow. (a) one single triangular surface and X is in shadow; (b) one single triangular surface and X is in sunlight; (c) multiple surfaces with varying interactions.

Formally, considering solar ray from the source along given direction in Eq (5), we can solve the intersection with

$$x_i + t_i L_i = p_{1i} + u_i(p_{3i} - p_{1i}) + v_i(p_{2i} - p_{1i}) \tag{6}$$

The intersection test yields real parameters u, v, t.

Based on Möller-Trumbore intersection algorithm [57], if and only if the real control parameters u, v, t satisfying

$$u, v, t > 0 \tag{7}$$

$$u + v \le 1 \tag{8}$$

$$0 \le t \le 1 \tag{9}$$

It is with shadow. The first inequality represents the intersection is between light source and point X. The second and third inequalities represent the intersection is inside the triangle surface. If all three conditions hold, the centroid point is shaded. Otherwise, it is sunlit. However, classical methods must repeat this intersection test for every triangle surface in the geometric model, which becomes computationally expensive and time consuming for large urban scale datasets with large amount of buildings.

2.2. Quantum annealing approach

To leverage the power of quantum annealing to solve this sunlit problem, we first define a binary variable

$$q = \begin{cases} 1, \textit{with shadow} \\ 0, \textit{in sunlight} \end{cases} \tag{10}$$

Then we reformulated the constraints in Eqs (7–9) using Big-M formulation [58] with the above binary variable q:

$$u > 0 \Leftrightarrow u > -M(1-q)$$

$$v > 0 \Leftrightarrow v > -M(1-q)$$

$$t \ge 0 \Leftrightarrow t \ge -M(1-q)$$

$$u + v \le 1 \Leftrightarrow u + v \le 1 + M(1-q)$$

$$t \le 1 \Leftrightarrow t \le 1 - M(1-q)$$

where M is a large enough constant. In this study, we set $M = 5000$.

Therefore, the optimization equation below determines whether solar rays are blocked or not by a triangle, as illustrated in Fig. 2(a) and Fig. 2(b)

$$\begin{aligned}
&\min_{q} -q\\
&s.t.\\
&t \geq -M(1-q)\\
&u > -M(1-q)\\
&v > -M(1-q)\\
&u+v \leq 1+M(1-q)\\
&t \leq 1+M(1-q)\\
&q \in \{0,1\}
\end{aligned} \tag{11}$$

The constraints in the above optimization are exactly converted from Möller-Trumbore intersection algorithm [57]. Optimization result of q = 1 indicates the shadow (blocked) condition in Fig. 2 (a), and optimization result of q = 0 indicates the illuminated (in sunlight) condition in Fig. 2 (b).

For multiple spatial triangles, such as two triangles shown in Fig. 2 (c), all the triangles must be considered simultaneously. We introduce another binary variable z to represent the combined status of all triangles:

$$z = \begin{cases} 1, \textit{with shadow} \\ 0, \textit{in sunlight} \end{cases} \tag{12}$$

The relationship between z and the set of q binary variables follows an OR logic. This means that as long as one triangle blocks the light, the point is considered in shadow. Only when all triangles fail to block the light is the point illuminated. Thus

$$z = \bigcup_i q_i \tag{13}$$

Where q_i is for the ith spatial triangle defined in Eq (10).

The OR logic calculation of the binary variables z and q_i in Eq. (13) can be expressed as

$$z \geq q_i$$

$$z \leq \sum_i q_i$$

Accordingly, the formulation to determine the status of one triangle in the presence of other i spatial triangles deduced from one triangle in Eq (11) is

$$\begin{aligned}
&\min_{q_i,z} \sum_i -q_i\\
&s.t.\\
&t_i \geq -M(1-q_i)\\
&u_i \geq -M(1-q_i)\\
&v_i \geq -M(1-q_i)\\
&u_i+v_i \leq 1+M(1-q_i)\\
&t_i \leq 1+M(1-q_i)\\
&z \geq q_i\\
&z \leq \sum_i q_i\\
&q_i \in \{0,1\}, z \in \{0,1\}
\end{aligned} \tag{14}$$

Since the constraints $z \geq q_i$ apply to all triangles, the number of the constraints equals the number of triangles. With a large number of surface triangles in the building models in space, solving optimization with all these constraints directly is still computationally expensive. To address this, we needed to simplify the constraints.

Note that

$$z \geq q_i \Leftrightarrow \min \sum_i q_i(1-z) \tag{15}$$

And the above relationship established based on binary relationship listed in Table 1.

Therefore, after simplifying the constraints in Eq (15) into the objective function in Eq (14), the objective function became quadratic form as

$$\min \sum_i -q_i + \sum_i q_i(1-z) = \min \sum_i -q_i z \tag{16}$$

Thus, the final formulation of the solar shadow problem is

$$\begin{aligned}
&\min_{q_i,z} \sum_i -q_i z\\
&s.t.\\
&t_i \geq -M(1-q_i)\\
&u_i \geq -M(1-q_i)\\
&v_i \geq -M(1-q_i)\\
&u_i+v_i \leq 1+M(1-q_i)\\
&z \leq \sum_i q_i\\
&q_i \in \{0,1\}, z \in \{0,1\}
\end{aligned} \tag{17}$$

Once the real control parameters u, v, t are solved, the status of the binary variable z can be determined by using quantum computing. This approach enables the optimization process by quantum annealing to handle a large number of surface triangles in surrounding buildings simultaneously.

Table 1
Binary relationship of $z \geq q_i$ and $\min \sum_i q_i(1-z)$.

z	q_i	$z \geq q_i$	$q_i(1-z)$	$\min q_i(1-z)$
0	0	Yes	0	Yes
0	1	No	1	No
1	0	Yes	0	Yes
1	1	Yes	0	Yes

2.3. Case study with the building models in San Francisco

To demonstrate and validate the feasibility of our developed quantum approach, we carried out a case study using the actual building models of San Francisco [55], shown in Fig. 3. The study area covered 1 km^2 and included about 5000 buildings.

Our quantum-based method requires surface triangulation as Fig. 2 illustrates. Based on building stories and thermal zones, each rectangular building surface was divided into triangles by drawing diagonals. Fig. 4 illustrates the building surface Delaunay triangulation for both commercial and residential buildings. After applying this process to all buildings, we obtained a total of 368,416 triangular surfaces for 5000 buildings in the area in Fig. 3(a).

For detailed analysis, we focused on one target building and considered possible shadow effects from surrounding building surfaces within a 50 m diameter, as shown in Fig. 3(b). This distance can also be adjusted depending on research needs and goal, building size, height, and type. The target building itself contained 52 triangular surfaces as shown in Fig. 4(a), while more than 2700 triangular surfaces were located in the surrounding buildings within the 50 m range.

To determine solar shadow conditions at various times in one day, solar angle data was also required. We obtained these data from the TMY data. With solar azimuth angle ϕ and solar altitude angle α in TMY data, the solar direction in Eq. (5) can be calculated based on the equations below.

$$\begin{aligned}
&l_x = \cos\alpha\sin\phi\\
&l_y = \cos\alpha\cos\phi\\
&l_z = \sin\alpha
\end{aligned}$$

Fig. 5 shows solar angles at different times on January 1st (winter) and July 1st (summer) in two days. On January 1st, daylight lasts from 8:00 to 17:00, while the rest of the time the sun angle is negative, indicating shadow. On July 1st, daylight extends from 6:00 to 19:00.

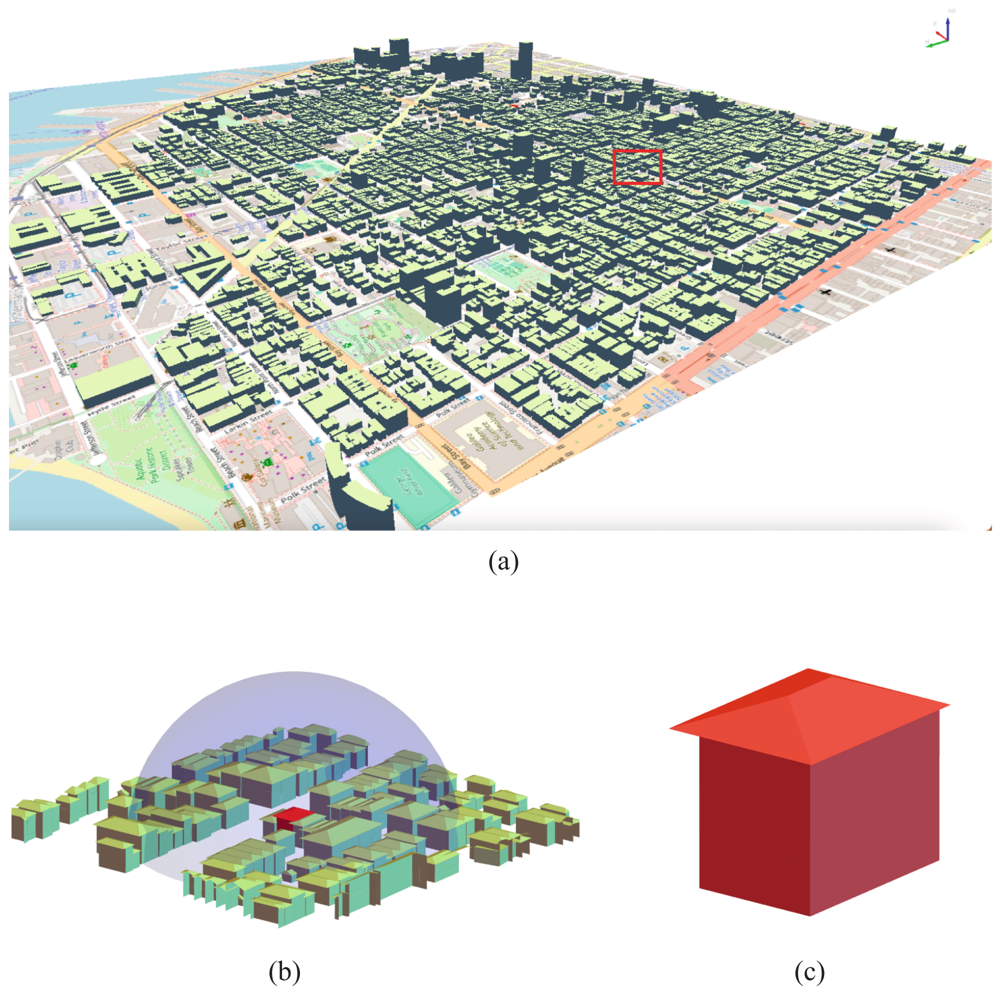

(a)

(b) (c)

Fig. 3. Building geometry model of about 5000 buildings and 368,416 surfaces in San Francisco for the case study. We zoomed in one district and marked one target building and 50 m diameter.

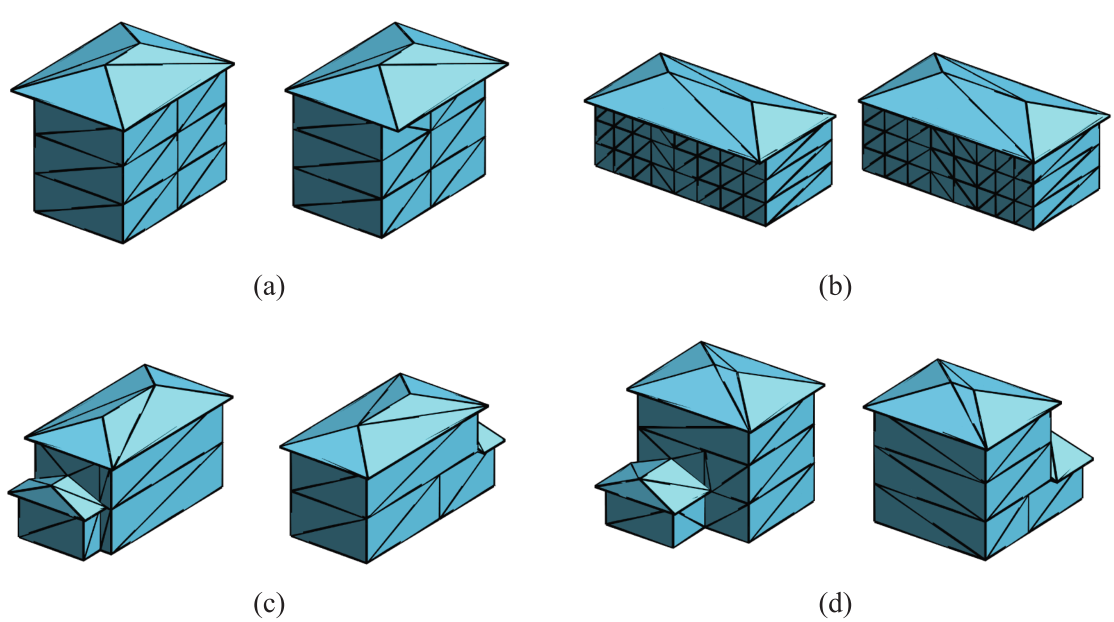

(a) (b)

(c) (d)

Fig. 4. Surface Triangulation of buildings (a) (b) commercial buildings; (c) (d) residential buildings.

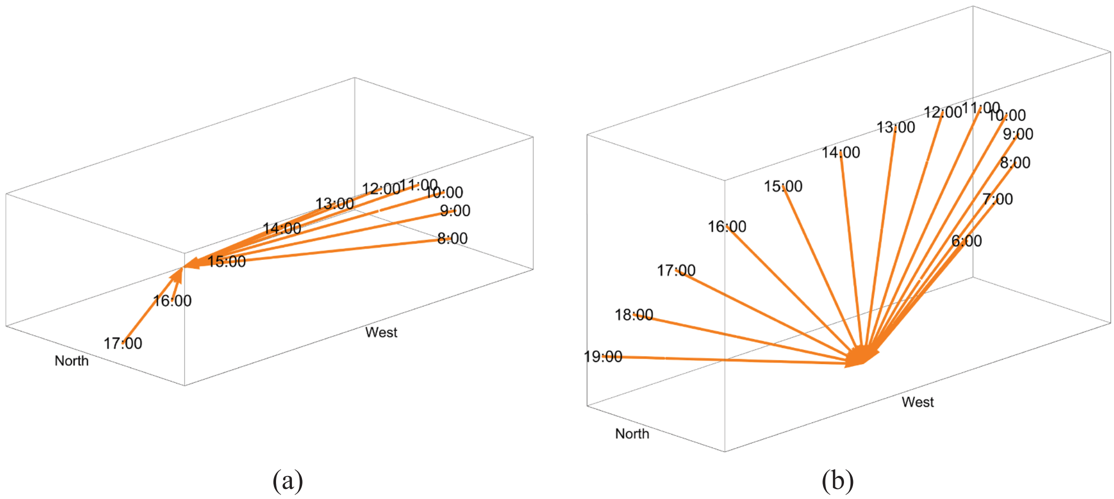

Fig. 5. Solar angle at different times in two days for case study: (a) January 1st. (b) July 1st.

2.4. Quantum computer configuration

We used the Advantage2 Quantum Computer from D-Wave, which features 4400 qubits and over 40,000 couplers [59]. Since the formulation in Eq. (17) includes constraints, we employed the Constrained Quadratic Model (CQM) in D-Wave quantum computer [60]. The general form of CQM is

$$\begin{aligned} &\min \sum_i a_i x_i + \sum_{ij} b_{ij} x_i x_j \\ &s.t. \sum_i a_i^m x_i + \sum_{ij} b_{ij}^m x_i x_j + c^m \leq 0 \end{aligned} \tag{18}$$

where x_i, x_j are binary variables, a_i, b_{ij}, a_i^m, b_{ij}^m, c^m are coefficients.

After preparing the building model data and solar angle data, we could prepare objective functions and constraints for quantum annealing. Based on Eq. (17), the linear coefficients of objective function were 0, while the quadratic coefficients of objective function were -1. These coefficients were mapped to nodes and edge weights within the Zephyr graph architecture of qubits on the D-Wave quantum computer using minor embedding [61]. The Zephyr topology provides 20-way qubit connectivity. The minimum annealing time was 5 ns, and the computing time limit for each calculation was 5 s in this study. After the quantum annealing process reached a low-energy solution of the Hamiltonian as Eq (1), the quantum computer returned samples of qubit states either 0 or 1. From these results and Eq (12), we determined the surface status whether illuminated or shadowed.

We used Python because the D-Wave Leap quantum computing cloud platform also uses Python as its programming language. The source code can be shared upon request and needed. To compare and validate the quantum computing results, we also used original Möller-Trumbore intersection algorithm of classical computing in Eqs (6–9) in this case study as benchmark.

3. Results

Fig. 6 shows the pie charts of qubit status for the 52 surfaces of a target building in the case study on January 1st at 8:00 am. From these qubit results, we can distinguish between surfaces "under light" and those "with shadow," as indicated in the figure. During this winter morning hour, most surfaces remain in shadow as the solar angle is low, with only four surfaces receiving direct sunlight.

We used quantum annealing to calculate the sunlit condition of all building surfaces. Fig. 7 presents both the distribution of quantum sample numbers and the proportion of accurate quantum samples for 52 surfaces of the target building in two days. The actual computing time was 4.11 s for each building surface on average. Quantum sample is one candidate solution returned by quantum annealer after finishing one

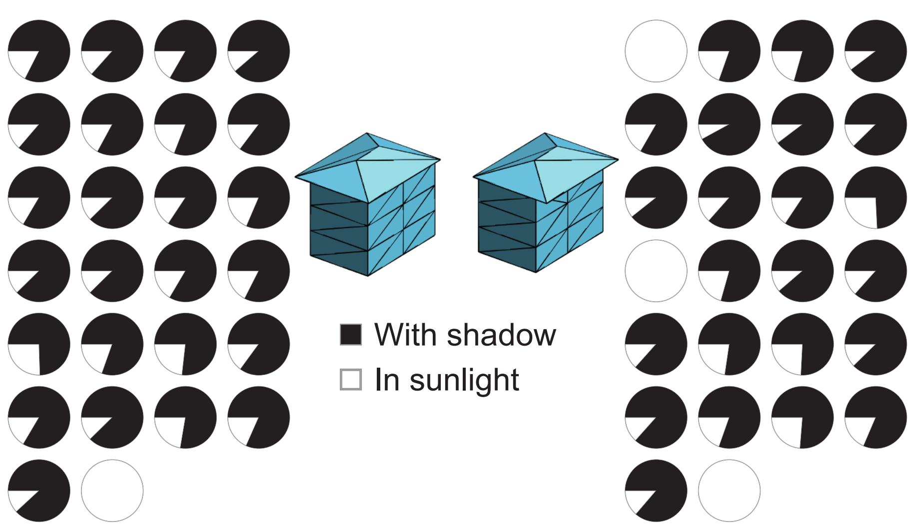

Fig. 6. Pie charts of qubit status for 52 surfaces of the target building on January 1st at 8am.

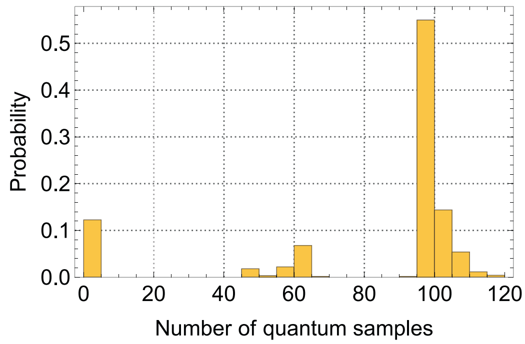

(a)

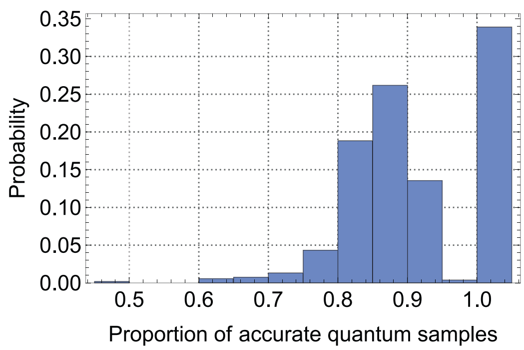

(b)

Fig. 7. Distribution of (a) number of quantum samples and (b) proportion of accurate quantum samples in computing time limit of 5 s.

calculation. In quantum computing, due to hardware noise and error rate, the correctness of results cannot be guaranteed for each run. We need to run the algorithm multiple times to obtain reliable results. For surfaces "with shadow" ($z = 1$), the quantum sampler produced around 100 samples, with an average of 91 samples within 4.11 s quantum computing time. This corresponded to about 0.045 s per sample. By contrast, for "in sunlight" cases ($z = 0$), the number of samples was much smaller and fewer than three. This was because these cases occur only when all surrounding surfaces fail to block sunlight ($q_i = 0$), which was relatively rare. On average, the proportion of accurate samples exceeded 92.4 %. Only one error was observed, and a single surface was miscalculated. Aside from this, the lowest accuracy observed for any case was above 60 %, demonstrating that the quantum samples are sufficiently reliable for this binary problem of solar shadow calculation in Eq. (17).

Figs. 8 and 9 illustrate the target building's surface conditions on January 1st (winter representative day) and July 1st (summer representative day), respectively. Orange color indicates sunlit surfaces, while black color indicates shaded ones. The result at 8am on Fig. 8 is also from Fig. 6. We found that quantum computing achieved 100 % and 99.86 % accuracy in winter and summer cases, respectively. The accuracy is measured by the number of correct quantum results compared with the results of traditional deterministic algorithms. The results show that in the morning the southeast surfaces are illuminated, at noon the roof receives the most sunlight, and in the evening the north-facing surfaces are lit. As the target building is surrounded by adjacent buildings on its east and west sides, its overall solar exposure is limited.

Fig. 10 shows the hourly sunlit fraction on surface area of the building by quantum computing at different times in four days in different seasons, and two days (Jan. 1st and July 1st) were shown as the results in Figs. 6, 8, 9. The duration of sunlight varies in different seasons. The surface sunlit fraction in Fig. 10 was calculated using the equation below

$$sunlit\ fraction = \frac{\sum_j Area_j \times z_j}{\sum_j Area_j} \tag{19}$$

Where $Area_j$ is the area of surface j, and z_j is defined in Eq (12) and calculated by quantum computing in Eq (17). We found that over the course of the day, about 40 % of the building surface is illuminated, but this fraction drops to around 30 % at noon. From this curve, the solar energy gain can be directly estimated from quantum computing, which is highly valuable for urban building energy modeling.

Considering large-scale urban energy simulations, the solar shadow results of this quantum computing can be directly output to energy simulation programs such as EnergyPlus via import of surface shading schedules [62]. As the calculation of sunlight shadow is independent of

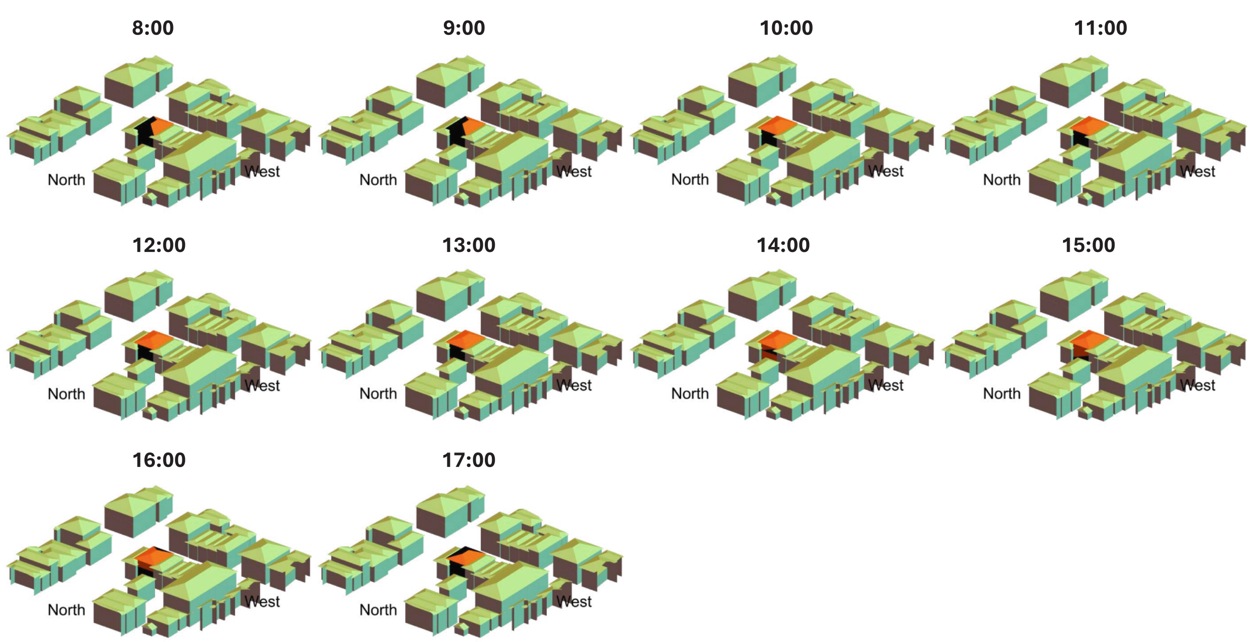

Fig. 8. Winter shadowing results of the target building with surrounding buildings at different times on January 1st. Orange color indicates sunlit surfaces, while black color indicates shaded ones. (For interpretation of the references to colour in this figure legend, the reader is referred to the web version of this article.)

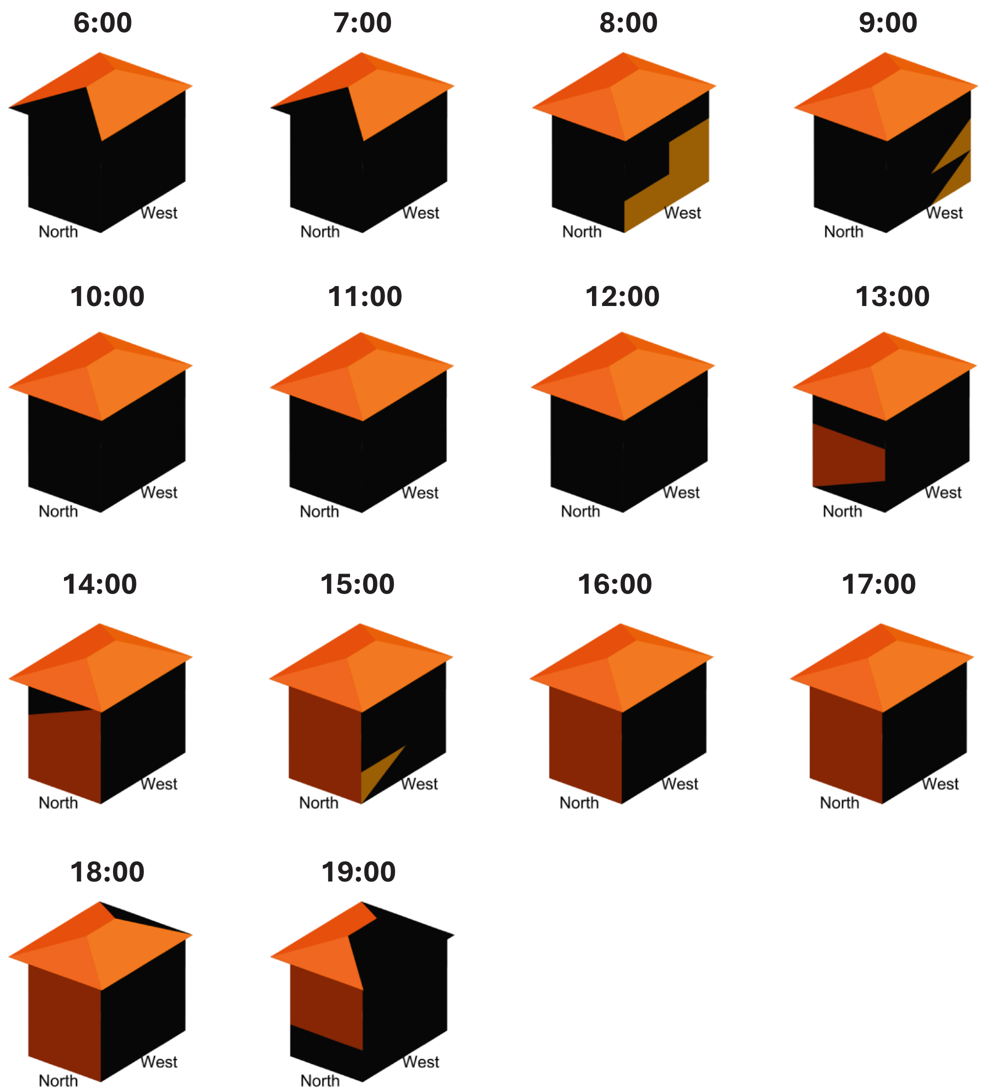

Fig. 9. Summer shadowing results of the target building at different times on July 1st. Orange color indicates sunlit surfaces, while black color indicates shaded ones. (For interpretation of the references to colour in this figure legend, the reader is referred to the web version of this article.)

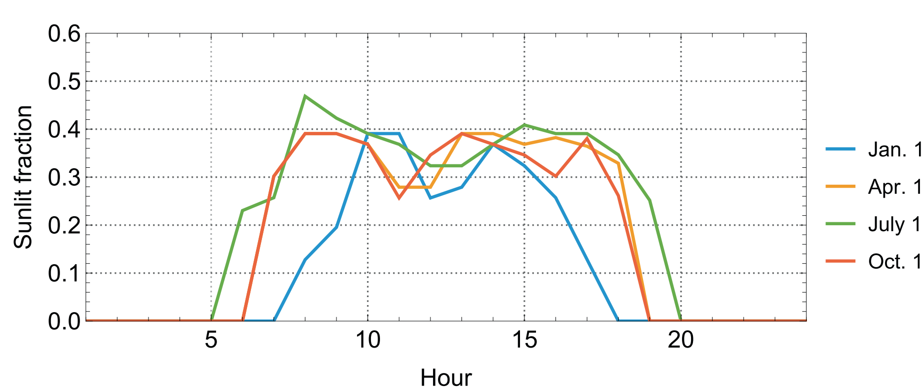

Fig. 10. Hourly sunlit fraction of the surface area of the target building at different times in four days in different seasons.

the energy simulation program and is only related to the building geometry and the solar angle. In addition, the quantum computing result can also be directly used to evaluate the power generation potential of rooftop solar panels [63,64], Building-Integrated Photovoltaics (BIPV) [65,66], and solar facades on urban buildings [67]. It can also be used to assess the necessity of installing shading in urban residential and outdoor areas [68]. There are wide range of application scenarios, and quantum computing is beneficial to the use of renewable energy and environmental comfort in cities.

4. Discussion

In this paper, we formulated the solar shadow calculation problem as a binary optimization model and solved it using quantum annealing. Two states "in sunlight" or "with shadow" can be represented by qubit superposition. To demonstrate and validate the feasibility of this approach, we conducted a case study using actual building models. The results showed high accuracy and promising scalability. However, the current implementation has limitations. First, in our urban building models, vegetation such as trees was excluded, even though trees play an important role in urban comfort and energy modeling [17,69]. Second, the geometric model did not consider terrain or topographic variations, which can influence solar radiation distribution [70]. We assumed that all building foundations lie on a flat plane, despite the fact that real urban environments, such as San Francisco, have significant elevation differences. This simplification may introduce discrepancies between the model and actual sunlit exposure on building surfaces. Third, we chose the value of big M to ensure that the constraints are met. From the high accuracy results (only one calculation error), the impact of this M value on the results in this paper is minimal. However, the impact of using different values on the quantum computing results is currently unknown. Some previous papers have mentioned the difficulty in determining the M value [71,72]. We think that reducing M value might affect the accuracy of the quantum computing results, which could be part of future benchmarking work and large-scale studies. Finally, our calculation of sunlit surfaces included only direct solar radiation and did not account for reflection. These limitations can be addressed and improved in future studies.

This work represents the first and new effort to apply quantum computing to building surface solar shadow analysis. The objective of this work was to explore the potential of quantum computing for this challenging and essential problem, and our findings indicated strong potential benefits. This study serves as a foundational step that informs future research directions. In particular, future work can investigate larger-scale problem instances involving multiple buildings on urban scale and develop benchmarking standards for this problem. Establishing benchmarks and time complexity analysis are essential for evaluating the effectiveness of quantum algorithms on new and complicated problems. For any given solar ray, many triangles and constraints do not actually intersect with it. In this work, however, we included all triangles to simplify implementation, allowing us to use a unified set of constraints and geometry for all solar-ray directions and for the quantum computing framework. Employing additional pre-screening algorithms would also increase computational time, particularly at large urban scales with many buildings. In future work, we can streamline the algorithm by considering only those triangles and constraints lying within the region and orientation relevant to a particular solar ray. This targeted selection has the potential to simplify optimization and improve both computational speed and accuracy.

Building on our approach, future study may address the following key research questions:

- How many qubits are required to perform solar shadow calculations for building models of various scales?
- What is the number of buildings we can compute in the current and future quantum computing hardware?
- What is the time complexity of the approach, and how can scalability be improved toward achieving quantum advantage?
- What is the relationship between the number of qubits, number of samples, and computational accuracy for solar shadow calculations?
- What size and number of triangulated building surfaces are practical and acceptable using quantum computing for further urban energy modeling?

Quantum annealing is an optimization technique rather than a deterministic algorithm with a fixed runtime bound. As a result, the computational complexity of quantum annealing on this problem is difficult to characterize theoretically. The performance depends on both the problem encoding and the annealing schedule [73]. And scaling behavior is typically evaluated empirically. Therefore, benchmarks are needed to compare computation time and efficiency against classical algorithms like ray tracing. Currently we may not have quantum supremacy for this problem. Continued increases in qubit capacity and improvements in quantum hardware in the future will enable larger problem sizes without proportional increases in computation time. Our future work also includes assessing whether the proposed approach can handle larger urban regions. Regarding quantum hardware limitations, current quantum solvers support a maximum of 500,000 binary variables and 100,000 constraints. However, a large number of variables and constraints are limited by queuing in the quantum cloud system to submit the program to solve and the use of traditional algorithm for decomposition. Therefore, it is indeed limited for very large-scale problems. But with future quantum hardware development, we believe the number of solvable variables and constraints will increase.

In this study, we focused on quantum annealing for solving binary variable problems. However, other quantum algorithms are also promising. For example, we can construct quantum circuits and investigate variational quantum algorithms [74], especially Quantum Approximate Optimization Algorithm (QAOA) [75]. It is another popular algorithm for optimization problems. Exploring QAOA for solar shadow calculations would be a valuable direction for future work. At present, quantum computing is most effective for problems expressed with binary variables and is less mature for continuous problems or systems of equations. For this reason, we used classical methods to solve linear equations and generate constraints. However, the Harrow-Hassidim-Lloyd (HHL) algorithm [76] provides a quantum method for solving linear systems. By coupling HHL, it may be possible to solve solar shadow and sunlit surface calculations entirely within a quantum computing framework completely.

5. Conclusion

The main conclusions of this study are listed below:

1) By converting "in sunlight" or "with shadow" into a binary variable (0/1) and representing it with qubit superposition, and applying surface triangulation together with the Möller–Trumbore intersection algorithm, solar shadow calculations can be formulated for quantum annealing.
2) Using real urban-scale building models and sunlight data, this study demonstrates the feasibility of applying quantum computing to solar shadow calculations. The method achieves nearly 100 % accuracy, shows strong scalability, and will benefit from reduced computation time as quantum hardware develops in the future.
3) This is the first study to apply quantum computing to the solar shadow and building surface sunlit problem. It introduces a new paradigm that differs fundamentally from traditional approaches such as ray tracing [6,15], Z-buffering [77], and parallel computing [14]. Establishing benchmarks is essential for evaluating the effectiveness of quantum algorithms for solar shadow calculation in the future.

CRediT authorship contribution statement

Zhipeng Deng: Writing – original draft, Validation, Software, Methodology, Conceptualization. **Yujie Xu:** Writing – original draft, Methodology, Data curation. **Tianzhen Hong:** Writing – review & editing, Methodology, Conceptualization.

Declaration of competing interest

The authors declare the following financial interests/personal relationships which may be considered as potential competing interests: Given his role as Executive Editor, Dr Tianzhen Hong had no involvement in the peer review of this article and had no access to information regarding its peer review. Full responsibility for the editorial process for this article was delegated to another journal editor.

Data availability

Data will be made available on request.

References

[1] P. Nejat, F. Jomehzadeh, M.M. Taheri, M. Gohari, M.Z.A. Majid, A global review of energy consumption, CO2 emissions and policy in the residential sector (with an overview of the top ten CO2 emitting countries), Renew. Sustain. Energy Rev. 43 (2015) 843–862.
[2] P.G. Loutzenhiser, H. Manz, C. Felsmann, P.A. Strachan, T.H. Frank, G.M. Maxwell, Empirical validation of models to compute solar irradiance on inclined surfaces for building energy simulation, Sol. Energy 81 (2) (2007) 254–267.
[3] A.P.D.A. Rocha, R.C. Oliveira, N. Mendes, Technical Review of Solar distribution Calculation Methods: Enhancing simulation Accuracy for High-Performance and Sustainable buildings, Buildings 15 (4) (2025) 578.
[4] E. Arens, T. Hoyt, X. Zhou, L. Huang, H. Zhang, S. Schiavon, Modeling the comfort effects of short-wave solar radiation indoors, Build. Environ. 88 (2015) 3–9.
[5] X. Cao, X. Dai, J. Liu, Building energy-consumption status worldwide and the state-of-the-art technologies for zero-energy buildings during the past decade, Energ. Buildings 128 (2016) 198–213.
[6] Luo, X., Tang, Y. H., & Hong, T. (2020). Efficient computation of surface sunlit fractions in urban-scale building modeling using ray-tracing techniques.
[7] X. Luo, T. Hong, Y.H. Tang, Modeling thermal interactions between buildings in an urban context, Energies 13 (9) (2020) 2382.
[8] Y. Chen, T. Hong, Impacts of building geometry modeling methods on the simulation results of urban building energy models, Appl. Energy 215 (2018) 717–735.
[9] Y. Han, J.E. Taylor, A.L. Pisello, Exploring mutual shading and mutual reflection inter-building effects on building energy performance, Appl. Energy 185 (2017) 1556–1564.
[10] M.C. Dubois, Solar shading and building energy use, Lund University 960480 (1997) 1–118.
[11] P.R. Tregenza, Mean daylight illuminance in rooms facing sunlit streets, Build. Environ. 30 (1) (1995) 83–89.
[12] F. Lindberg, C.S.B. Grimmond, A. Martilli, Sunlit fractions on urban facets–Impact of spatial resolution and approach, Urban Clim. 12 (2015) 65–84.
[13] L. Bellia, C. Marino, F. Minichiello, A. Pedace, An overview on solar shading systems for buildings, Energy Procedia 62 (2014) 309–317.
[14] X. Zhou, X. Shen, Z. Liu, H. Sun, J. An, D. Yan, A novel shadow calculation approach based on multithreaded parallel computing, Energ. Buildings 312 (2024) 114237.
[15] S. Rayegan, M. Mortezazadeh, D. Zhan, A. Katal, L.L. Wang, R. Zmeureanu, S. Ranjbar, Development of a 3D ray tracing-based direct solar shading model for urban building energy simulation, Renew. Energy 256 (2026) 123883.
[16] Pan, J., & Jakubiec, J. A. (2022). Simulating the impact of deciduous trees on energy, daylight, and visual comfort: impact analysis and a practical framework for implementation. In Proceedings of ESim 2022: 12th conference of IBPSA-Canada, IBPSA Publications, Toronto.
[17] B. Tian, R.C.G.M. Loonen, J.L.M. Hensen, Combining point cloud and surface methods for modeling partial shading impacts of trees on urban solar irradiance, Energ. Buildings 298 (2023) 113420.
[18] S. Freitas, C. Catita, P. Redweik, M.C. Brito, Modelling solar potential in the urban environment: State-of-the-art review, Renew. Sustain. Energy Rev. 41 (2015) 915–931.
[19] A.K. Adeleke, J.L. Smit, Intergration of LIDAR data with aerial imagery for estimating rooftop solar photovoltaic potentials in city of cape town, Int. Arch. Photogramm. Remote. Sens. Spat. Inf. Sci. 41 (2016) 617–624.
[20] Wolk, S., Berzolla, Z., Carethers, L., & Reinhart, C. (2023, September). Accelerating photovoltaic potential simulations for urban building energy modeling to inform policymakers. In Building Simulation 2023 (Vol. 18, pp. 2628-2635). IBPSA.
[21] Z. Liu, X. Zhou, X. Shen, H. Sun, D. Yan, A novel acceleration approach to shadow calculation based on sunlight channel for urban building energy modeling, Energ. Buildings 315 (2024) 114244.
[22] S. Wang, R. Zhu, Y. Pu, M.S. Wong, Y. Xu, Z. Qin, Modelling sunlight and shading distribution on 3D trees and buildings: deep learning augmented geospatial data construction from street view images, Build. Environ. 275 (2025) 112816.
[23] E.G. Rieffel, A.A. Asanjan, M.S. Alam, N. Anand, D.E.B. Neira, S. Block, R. Biswas, Assessing and advancing the potential of quantum computing: a NASA case study, Futur. Gener. Comput. Syst. 160 (2024) 598–618.
[24] A. Ajagekar, F. You, Quantum computing for energy systems optimization: challenges and opportunities, Energy 179 (2019) 76–89.
[25] T. Hong, Y. Chen, X. Luo, N. Luo, S.H. Lee, Ten questions on urban building energy modeling, Build. Environ. 168 (2020) 106508.
[26] C. Thai, J. Brouwer, Challenges estimating distributed solar potential with utilization factors: California universities case study, Appl. Energy 282 (2021) 116209.
[27] M. Dorman, E. Erell, A. Vulkan, I. Kloog, shadow: R Package for Geometric Shadow Calculations in an Urban Environment, R J. 11 (1) (2019) 287.
[28] I. Maestre, L. Pérez-Lombard, J. Foncubierta, P. Cubillas, Improving direct solar shading calculations within building energy simulation tools, J. Build. Perform. Simul. 6 (6) (2013) 437–448.
[29] EnergyPlus Team, "Shading Module: Engineering Reference — EnergyPlus 25.1." Accessed: Sep. 25, 2025. [Online]. Available: https://bigladdersoftware.com/epx/docs/25-1/engineering-reference/shading-module.html.
[30] B. Tian, R.C. Loonen, Á. Bognár, J.L. Hensen, Impacts of surface model generation approaches on raytracing-based solar potential estimation in urban areas, Renew. Energy 198 (2022) 804–824.
[31] R. Goldstein, K. Walmsley, N. Morris, A. Tessier, in: May). Algorithms for Voxel-Based Architectural Space Analysis, IEEE Computer Society, 2023, pp. 508–519.
[32] J. Liang, J. Gong, A sparse voxel octree-based framework for computing solar radiation using 3d city models, ISPRS Int. J. Geo Inf. 6 (4) (2017) 106.
[33] S. Anselmo, M. Ferrara, Trends and evolution of the GIS-based photovoltaic potential calculation, Energies 16 (23) (2023) 7760.
[34] E.G. Melo, M.P. Almeida, R. Zilles, J.A. Grimoni, Using a shading matrix to estimate the shading factor and the irradiation in a three-dimensional model of a receiving surface in an urban environment, Sol. Energy 92 (2013) 15–25.
[35] M. Karteris, T. Slini, A.M. Papadopoulos, Urban solar energy potential in Greece: a statistical calculation model of suitable built roof areas for photovoltaics, Energ. Buildings 62 (2013) 459–468.
[36] J. Liang, J. Gong, W. Li, A.N. Ibrahim, A visualization-oriented 3D method for efficient computation of urban solar radiation based on 3D–2D surface mapping, Int. J. Geogr. Inf. Sci. 28 (4) (2014) 780–798.
[37] H. Lan, Z. Gou, C. Hou, Understanding the relationship between urban morphology and solar potential in mixed-use neighborhoods using machine learning algorithms, Sustain. Cities Soc. 87 (2022) 104225.
[38] G. Li, Z. Wang, C. Xu, T. Li, J. Gao, Q. Mao, S. Chen, A district-scale spatial distribution evaluation method of rooftop solar energy potential based on deep learning, Sol. Energy 268 (2024) 112282.
[39] C. Alves, L.P. Santos, T. Bashford-Rogers, in: November). A Quantum Algorithm for Ray Casting Using an Orthographic Camera, IEEE, 2019, pp. 56–63.
[40] L.P. Santos, T. Bashford-Rogers, J. Barbosa, P. Navrátil, Towards quantum ray tracing, IEEE Trans. Vis. Comput. Graph. 31 (4) (2024) 2223–2234.
[41] Lu, X., & Lin, H. (2022). A framework for quantum ray tracing. arXiv preprint arXiv:2203.15451.
[42] L. Mosier, M. McGuire, T. Hachisuka, December). Quantum Ray Marching: Reformulating Light Transport for Quantum Computers, in: In SIGGRAPH Asia 2023 Conference Papers, 2023, pp. 1–9.
[43] I. Wald, V. Havran, in: September). on Building Fast Kd-Trees for Ray Tracing, and on Doing That in O (n Log n), IEEE, 2006, pp. 61–69.
[44] X. Lu, H. Lin, Improved quantum supersampling for quantum ray tracing, Quantum Inf. Process 22 (10) (2023) 359.
[45] I. Hen, F.M. Spedalieri, Quantum annealing for constrained optimization, Phys. Rev. Appl 5 (3) (2016) 034007.
[46] T. Kadowaki, H. Nishimori, Quantum annealing in the transverse Ising model, Phys. Rev. E 58 (5) (1998) 5355.
[47] A. Abbas, A. Ambainis, B. Augustino, A. Bärtschi, H. Buhrman, C. Coffrin, C. Zoufal, Challenges and opportunities in quantum optimization, Nat. Rev. Phys. (2024) 1–18.
[48] A. Lucas, Ising formulations of many NP problems, Front. Phys. 2 (2014) 5.
[49] M. Hoffmann, B.U. Schyska, J. Bartels, T. Pelser, J. Behrens, M. Wetzel, D. Stolten, A review of mixed-integer linear formulations for framework-based energy system models, Adv. Appl. Energy 100190 (2024).
[50] Z. Deng, X. Wang, B. Dong, Quantum computing for future real-time building HVAC controls, Appl. Energy 334 (2023) 120621.
[51] A. Ajagekar, F. You, Variational quantum circuit learning-enabled robust optimization for AI data center energy control and decarbonization, Adv. Appl. Energy 14 (2024) 100179.
[52] Z. Deng, B. Dong, September). Discrete Optimal Control of Building to Grid Integration Based on Quantum Computing Vol. 18 (2023) 2768–2775.
[53] Deng, Z., Wang, X., & Dong, B. (2025, February). Integrating quantum computing into building-to-grid control framework: Application of benders decomposition in mixed-integer nonlinear programming. In Building Simulation (pp. 1-16). Beijing: Tsinghua University Press.
[54] Z. Deng, Y. Li, X. Wang, Z. Jiang, B. Dong, Quantum computing-enhanced large-scale residential electric vehicle charging management, Appl. Energy 401 (2025) 126772.
[55] T. Hong, Y. Chen, S.H. Lee, M.A. Piette, CityBES: a web-based platform to support city-scale building energy efficiency, Urban Computing 14 (2016) 2016.
[56] M.A. Nielsen, I.L. Chuang, Quantum computation and quantum information, Cambridge University Press, 2010.
[57] T. Möller, B. Trumbore, Fast, minimum storage ray/triangle intersection. In ACM SIGGRAPH 2005 Courses, 2005.
[58] I. Griva, S.G. Nash, A. Sofer, Linear and nonlinear optimization, 2nd edition., Society for Industrial and Applied Mathematics, 2008.
[59] https://www.dwavequantum.com/media/wakjcpsf/adv2_4400q_whitepaper-1.pdf.
[60] https://docs.dwavequantum.com/en/latest/concepts/models.html.
[61] S. Okada, M. Ohzeki, M. Terabe, S. Taguchi, Improving solutions by embedding larger subproblems in a D-Wave quantum annealer, Sci. Rep. 9 (1) (2019) 2098.

[62] G. Ramos, E. Ghisi, Analysis of daylight calculated using the EnergyPlus programme, Renew. Sustain. Energy Rev. 14 (7) (2010) 1948–1958.

[63] M. Horváth, D. Kassai-Szoó, T. Csoknyai, Solar energy potential of roofs on urban level based on building typology, Energ. Buildings 111 (2016) 278–289.

[64] Y. Li, D. Ding, C. Liu, C. Wang, A pixel-based approach to estimation of solar energy potential on building roofs, Energ. Buildings 129 (2016) 563–573.

[65] N. Jakica, State-of-the-art review of solar design tools and methods for assessing daylighting and solar potential for building-integrated photovoltaics, Renew. Sustain. Energy Rev. 81 (2018) 1296–1328.

[66] K. Fath, J. Stengel, W. Sprenger, H.R. Wilson, F. Schultmann, T.E. Kuhn, A method for predicting the economic potential of (building-integrated) photovoltaics in urban areas based on hourly Radiance simulations, Sol. Energy 116 (2015) 357–370.

[67] P. Redweik, C. Catita, M. Brito, Solar energy potential on roofs and facades in an urban landscape, Sol. Energy 97 (2013) 332–341.

[68] I. Lee, J.A. Voogt, T.J. Gillespie, Analysis and comparison of shading strategies to increase human thermal comfort in urban areas, Atmos. 9 (3) (2018) 91.

[69] P. Balakrishnan, J.A. Jakubiec, Trees in daylight simulation–measuring and modelling realistic light transmittance through trees, Leukos 19 (3) (2023) 241–268.

[70] W. Liu, H. Guan, H.A. Gutiérrez-Jurado, E.W. Banks, X. He, X. Zhang, Modelling quasi-three-dimensional distribution of solar irradiance on complex terrain, Environ. Model. Software 149 (2022) 105293.

[71] M. Cococcioni, L. Fiaschi, The Big-M method with the numerical infinite M, Optim. Lett. 15 (7) (2021) 2455–2468.

[72] T. Kleinert, M. Labbé, F.A. Plein, M. Schmidt, There's no free lunch: on the hardness of choosing a correct big-M in bilevel optimization, Oper. Res. 68 (6) (2020) 1716–1721.

[73] P. Hauke, H.G. Katzgraber, W. Lechner, H. Nishimori, W.D. Oliver, Perspectives of quantum annealing: Methods and implementations, Rep. Prog. Phys. 83 (5) (2020) 054401.

[74] M. Cerezo, A. Arrasmith, R. Babbush, S.C. Benjamin, S. Endo, K. Fujii, P.J. Coles, Variational quantum algorithms, Nat. Rev. Phys. 3 (9) (2021) 625–644.

[75] J. Choi, J. Kim, in: October). A Tutorial on Quantum Approximate Optimization Algorithm (QAOA): Fundamentals and Applications, IEEE, 2019, pp. 138–142.

[76] A.W. Harrow, A. Hassidim, S. Lloyd, Quantum algorithm for linear systems of equations, Phys. Rev. Lett. 103 (15) (2009) 150502.

[77] A.P. de Almeida Rocha, A. Rodler, R.C. Oliveira, J. Virgone, N. Mendes, A pixel counting technique for sun patch assessment within building enclosures, Sol. Energy 184 (2019) 173–186.